SUPPLEMENTAL INFORMATION

Multiscale QM/MM Molecular Dynamics Simulations of the Trimeric Major Light-Harvesting Complex II

Sayan Maity,[†] Vangelis Daskalakis,[‡] Marcus Elstner,[¶,§] and Ulrich Kleinekathöfer[*,†]

[†]*Department of Physics and Earth Sciences, Jacobs University Bremen, Campus Ring 1, 28759 Bremen, Germany*

[‡]*Department of Chemical Engineering, Cyprus University of Technology, 30 Archbishop Kyprianou Str. 3603, Limassol, Cyprus*

[¶]*Institute of Physical Chemistry, Karlsruhe Institute of Technology (KIT), Kaiserstrasse 12, 76131 Karlsruhe, Germany*

[§]*Institute of Biological Interfaces (IBG2), Karlsruhe Institute of Technology (KIT), Kaiserstrasse 12, 76131 Karlsruhe, Germany*

E-mail: u.kleinekathoefer@jacobs-university.de

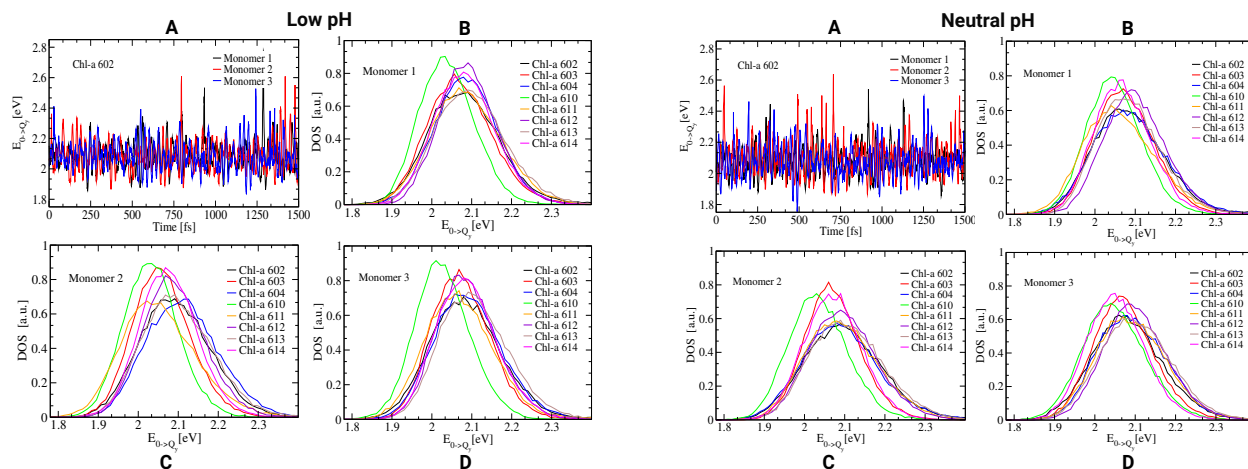# S1 Site Energy Distributions for the Individual Chl-a Pigments

Figure S1: Calculations at low and neutral lumenal pH values are shown in the left and right panels, respectively. A) Excited state calculation based on the TD-LC-DFTB approach along a piece of a QM/MM MD trajectory. B-D) Density of states for the individual Chl-a molecules in different monomers. Here the first set of the 40 ps QM/MM MD trajectories is shown.
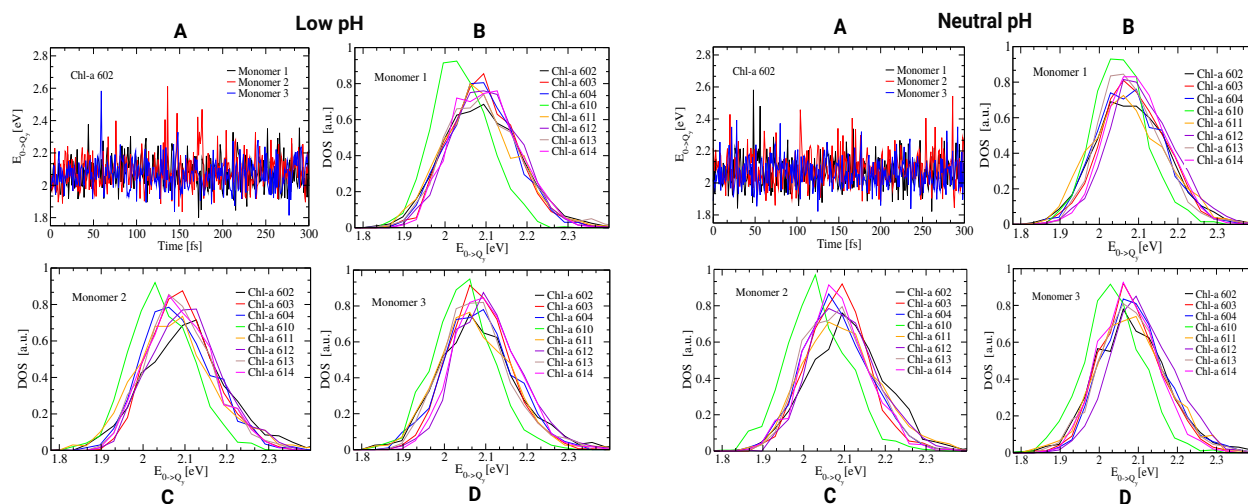

Figure S2: Same as Fig. S1 but based on 1 ns QM/MM MD trajectories.

S2   Autocorrelation Functions and Spectral Densities for the Individual Chl-a Pigments
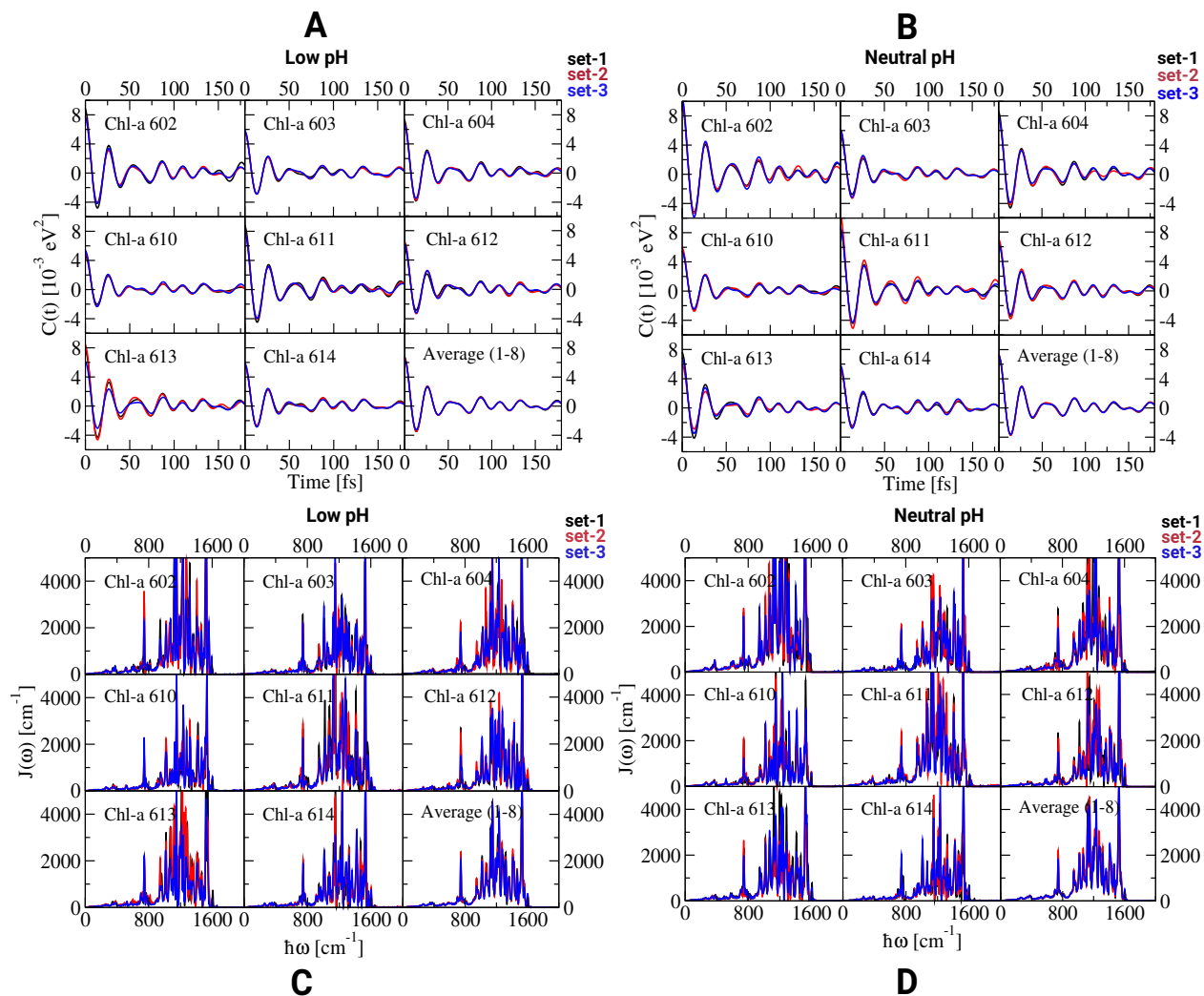

Figure S3: A, B) Average autocorrelation functions for the individual Chl-a pigments from different starting geometries at low and neutral lumenal pH. C,D) The respective spectral densities based on the autocorrelation functions.
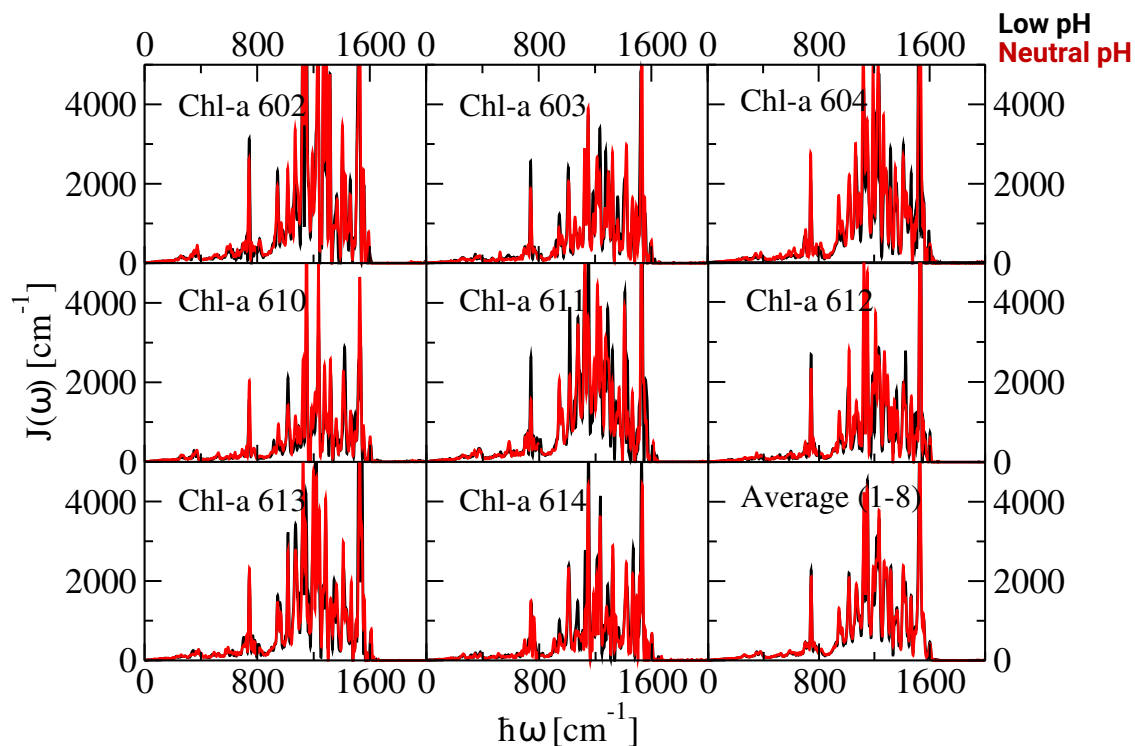
Figure S4: Spectral density comparison for each Chl-a at low and neutral pH state based on the first set of 40 ps QM/MM MD trajectory.

Table S1: Reorganization energies corresponding to the individual Chl-a pigments averaged over all three sets of QM/MM MD trajectories at both pH states.

Pigment	Low pH (cm^{-1})	Neutral pH (cm^{-1})
Chl-a 602	1266	1568
Chl-a 603	910	927
Chl-a 604	1110	1271
Chl-a 610	787	879
Chl-a 611	1264	1427
Chl-a 612	972	1046
Chl-a 613	1167	1079
Chl-a 614	895	856

S3 Comparison of Experimental Spectral Density with Different Broadening Parameter
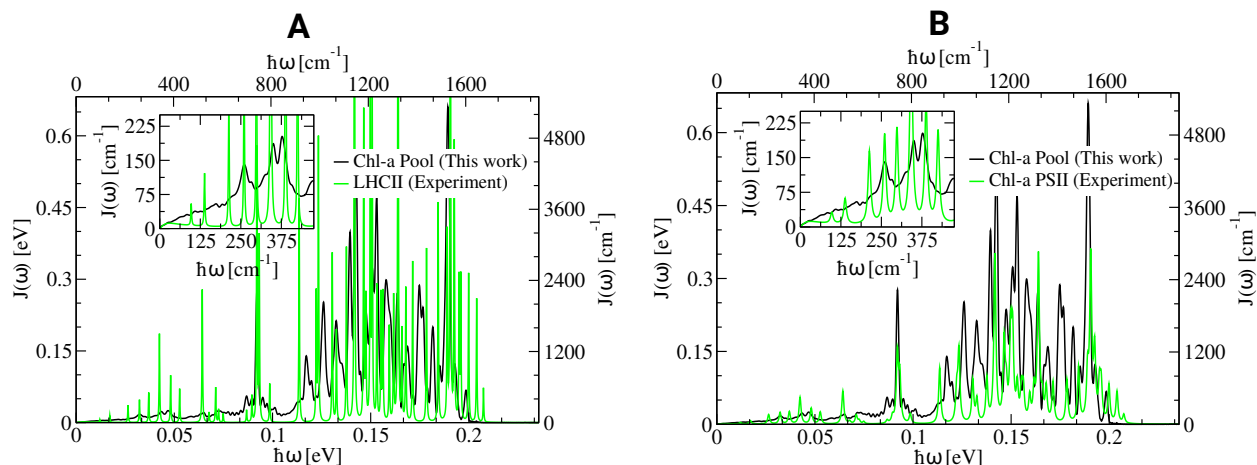
Figure S5: A) Comparison between the computed and the experimental spectral density as shown in the main text with the broadening parameter set to 3 cm^{-1} as given in the Ref. 1. B) Same as panel A but now the experimental spectral density is measured for the PSII complex[2] with a broadening parameter of 10 cm^{-1} as given in Refs. 3,4.

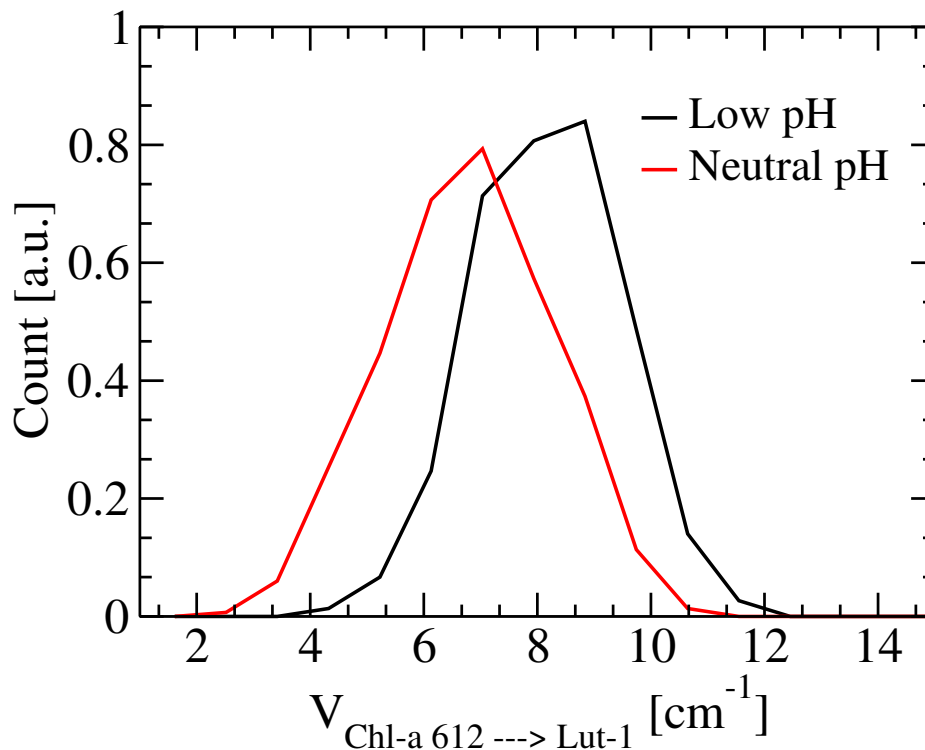## S4 Excitonic Coupling between Chl-a 612/Lut-1 Pair

Figure S6: Excitonic coupling distribution between Chl-a 612/Lut-1 pair at low and neutral pH states. These data are extracted from our previous study based on a 500 ns classical MD trajectory[5] but here they are scaled with a screening factor as explained in the main text.

References

(1) Novoderezhkin, V.; Palacios, M. A.; van Amerongen, H.; van Grondelle, R. Energy-Transfer Dynamics in the LHCII Complex of Higher Plants: Modified Redfield Approach. *J. Phys. Chem. B* **2004**, *108*, 10363.

(2) Bennett, D. I.; Amarnath, K.; Fleming, G. R. A Structure-Based Model of Energy Transfer Reveals the Principles of Light Harvesting in Photosystem II Supercomplexes. *J. Am. Chem. Soc.* **2013**, *135*, 9164–9173.

(3) Kreisbeck, C.; Kramer, T.; Aspuru-Guzik, A. Scalable High-Performance Algorithm for the Simulation of Exciton Dynamics. Application to the Light-Harvesting Complex II in the Presence of Resonant Vibrational Modes. *J. Chem. Theory Comput.* **2014**, *10*, 4045–4054.

(4) Bhattacharyya, P.; Fleming, G. R. The Role of Resonant Nuclear Modes in Vibrationally Assisted Energy Transport: The LHCII Complex. *J. Chem. Phys.* **2020**, *153*, 044119.

(5) Daskalakis, V.; Maity, S.; Hart, C. L.; Stergiannakos, T.; Duffy, C. D. P.; Kleinekathöfer, U. Structural Basis for Allosteric Regulation in the Major Antenna Trimer of Photosystem II. *J. Phys. Chem. B* **2019**, *123*, 9609–9615.